Increased Phosphorylation of Ca^{2+} Handling Protein as a Proarrhythmic Mechanism in Myocarditis

Hyelim Park

Department of Medical Science
The Graduate School, Yonsei University

Increased Phosphorylation of Ca^{2+} Handling Protein as a Proarrhythmic Mechanism in Myocarditis

The Master's Thesis
Submitted to the Department of Medical Science
the Graduate School of Yonsei University
in partial fulfillment of the
requirements for the degree of
Master of Medical Science

Hyelim Park

December 2013

This certifies that the Master's Thesis of Hyelim Park is approved.

_____

Thesis Supervisor: Boyoung Joung

_____

Thesis Committee Member #1: Young-Ho Lee

_____

Thesis Committee Member #2 : Sungha Park

The Graduate School
Yonsei University

December 2013

ACKNOWLEDGEMENTS

2011 년 9 월 저는 대학원 생활을 시작하였습니다. 그리고 약 2 년 뒤, 지금 저는 감사의 글을 쓰고 있습니다. 최선을 다해 보낸 지난 2 년여의 노력이 이렇게 소중한 결실을 보게 되어 매우 기쁘고 설렙니다.

지난 2 년여의 시간은 무엇 하나 만만한 것이 없었습니다. 하지만 그것을 빨리 인정하고 수용했기 때문에 겸손하고 치열한 자세로 공부할 수 있었고, 지금의 결실도 볼 수 있었습니다. 그리고 석사학위라는 학문적 성과 뿐만 아니라, 인생을 살아가는 중요한 가르침도 얻었고, 그 동안 도움을 준 많은 분들께 진심으로 감사해야 함을 배웠습니다. 그리고 그 첫 실천으로 이번 석사학위 속 감사의 글을 통해 제게 은혜를 주신 분들께 감사의 마음을 전하고자 합니다.

무엇보다도 항상 딸에게 칭찬만 해주시고 제 편으로 든든하게 계셔주신 아빠, 언제나 따뜻하게 사랑해주시고 저의 결정을 지지해주시는 엄마, 자신도 같은 연구실에서 공부를 하면서도 언제나 제게 신경을 써준 동생 혜원에게 진심으로 감사의 말씀을 전합니다. 저희 가족 외에도 언제나 따뜻하게 대해주시는 할아버지,할머니, 항상 뵐 때마다 정을 느끼게 해주시는 이모께도 감사의 말씀을 올립니다.

특히 지도교수님이신 정보영 교수님은 제 인생의 가장 커다란 선물이었음을 고백합니다. 열정적인 지도는 저를 많이도 겸손하게 해주었고, 열정적인 랩미팅과 학생들과의 소통을 통해 많은 가르침을 받았습니다. 또한 개인적으로는 부족하지만 여러 번의 기회를 통해 APHRS 와 대한심장학회 등에서 발표와 수상 같은 소중한 경험을 쌓을 수 있었습니다. 진심으로 감사한 마음을 갖고 살아가겠습니다.

논문 심사과정에서 심사를 맡아 주신 이영호 교수님, 박성하 교수님의 세심한 제안은 연구자로서 더욱 깊은 사고를 할 수 있도록 해주었습니다. 깊은 감사를 드립니다.

연세대학교 대학원에서 많은 사람들을 만날 수 있었습니다. 언제나 친언니처럼 관심 가져주시고 격려해 주신 현주언니, 이 논문의 주제인 심근염 모델 연관 자료들을 모두 찾아주고 실험을 하는데 많은 조언을 아끼지 않은 다정언니가 없었다면 논문을 작성하는 시간은 훨씬 더 걸렸을 것으로 생각됩니다. 그리고 오래 보지는 못했지만 언제나 기운을 전해준 보형언니, 부탁이 있을 때마다 언제든지 달려와서 도와준 이범섭님, 저를 응원해주고 연구에 많은 기여를 하고 있는 오수정. 진심으로 감사의 말씀을 전합니다.

오래된 친구인 언제나 반갑게 맞이하고 즐거운 시간을 만들어주는 채순영,이다혜, 장혜경, 진심으로 저를 신뢰하고 지지해준 존재만으로 소중한 노현주에게 감사드립니다.

막상 감사의 글을 적고 나니 이렇게 많은 분들의 격려와 도움 속에서 석사과정을 마쳤다는 생각에 감사한 마음이 가득해집니다. 학교에서 보낸 지난 시간들은 앞으로의 제 인생에서 많은 영향을 미치게 될 것으로

생각됩니다. 그 동안 도움 주신 분들께 다시 한번 감사드리며 이번 석사과정이 학업의 끝이 아니고 시작일 뿐이라고 굳게 다짐해봅니다.

앞으로 세상에 보탬이 되고 즐거움을 줄 수 있는 사람이 될 수 있도록 끊임없이 노력하고 정진하겠습니다. 감사합니다.

2013.12

TABLE OF CONTENTS

LIST OF FIGURES

ABSTRACT

Increased Phosphorylation of Ca^{2+} Handling Protein as a Proarrhythmic Mechanism in Myocarditis

Hyelim Park

Department of Medical Science

***The Graduate School,* Yonsei University**

(Directed by Professor Boyoung Joung)

Fatal arrhythmia is an important cause of death in patients with myocarditis. This study investigated the proarrhythmic mechanisms of experimental autoimmune myocarditis (EAM). EAM was induced by the injection of porcine cardiac myosin of 2 mg into footpads of adult Lewis rats on day 1 and 8 (Myo, n=15) and compared with control rats (Control, n=15). In additional rats, corticosteroid of 6 mg was injected into the gluteus muscle before the injection of porcine cardiac myosin on day 1 and 8 (MyoS, n=15). Myocytes with myocarditis produced by TNF-α treatment used in intracellular calcium measurement. Myocarditis hearts had longer action potential duration (APD),

slower conduction velocity (CV; $p<0.01$ versus control), steeper CV restitution kinetics, greater fibrosis, higher levels of transcripts for HMGB1, IL-6, and TNF-α and phosphorylation of Ca^{2+}/calmodulin-dependent protein kinase II (CAMKII), ryanodine receptor type 2 (RyR2) and phospholamban(PLB). Steroid treatment reversed the transcripts for myocarditis, flattened CV restitution kinetics, reduced APD at 90% recovery to baseline, increased CV ($p<0.01$), and reversed fibrosis and phosphorylation of CaMKII, RyR2 and PLB ($p<0.05$). Programmed stimulation triggered sustained VT in Myo (n=4/5), but not in control (n=0/5), and steroid (n=0/5, $p<0.001$) and CaMKII inhibitor (KN93) pretreatment (n=0/4, $p=0.001$). Myocytes with myocarditis had increased intracellular calcium ($p<0.01$ versus control), which was reversed by pretreatment with steroid and KN93. The electrophysiologic characteristics of myocarditis were increased APD, slower CV and steeper CV restitution kinetics. These changes might be related with calcium overloading by increased phosphorylation of CaMKII.

Key Words: myocarditis, arrhythmia, inflammation, Ca^{2+}/calmodulin-dependent protein kinase II

I. Introduction

Myocarditis and subsequent dilated cardiomyopathy (DCM) are major causes of heart failure and arrhythmia in young patients.[1] This condition is characterized by infiltration of inflammatory cells into the myocardium with consequent loss of myocytes and development of fibrosis and necrosis.[2] In a significant fraction of patients, the loss of cardiomyocytes leads to ventricular remodeling, permanent ventricular wall dysfunction, DCM, heart failure, and/or arrhythmias. Therefore, the understanding the mechanism of the ventricular arrhythmias in myocarditis is important in order to improve the treatment and patient′s prognosis.[3]

Experimental autoimmune myocarditis (EAM) in the rat is a unique and useful model for understanding myocarditis and subsequent DCM.[4] EAM rats exhibited high inducibility of ventricular arrhythmia and prolonged action potential duration (APD). However, the mechanism of arrhythmia was not fully evaluated. Inflammation of the heart, which is an important mechanism of myocarditis, increases oxidative stress. Oxidative stress can activate Ca^{2+}/calmodulin-dependent protein kinase II (CaMKII)[5], prolongs APD and induces afterdepolarization in cardiomyocytes.[6] Therefore, we hypothesized that the EAM-induced arrhythmia could be related with CaMKII activation, which was caused by the inflammation and oxidative stress. To prove this hypothesis, we evaluated arrhythmic events and survival in EAM model. Secondly, arrhythmic mechanisms of EAM model were studied in Langendorff-perfused isolated hearts. Thirdly, we evaluated whether the level of inflammation and CaMKII activation are increased in myocarditis. Finally, we investigated whether the arrhythmic events and

CaMKII activation were suppressed by pretreatment with an anti-inflammatory agent, corticosteroid.

Ⅱ. Methods

1. Induction of EAM

The investigation conforms to the *Guide for the Care and Use of Laboratory Animals* published by the US National Institutes of Health (NIH Publication, 8th Edition, 2011). This study protocol was approved by the Institutional Animal Care and Use Committee of Yonsei University College of Medicine and Cardiovascular Research Institute (Approval reference number 2011-0136), and conforms to the guidelines of the American Heart Association.

The EAM model was produced by the method described by Inomata et al.[7] Briefly, to induce inflammation, we used purified cardiac myosin (Sigma Aldrich, Schnelldorf, Germany) from porcine ventricular muscle as the antigen. Purified cardiac myosin at a concentration of 7 mg/ml was emulsified with an equal volume of complete Freund's adjuvant (BD biosciences, Heidelberg, Germany) supplemented with mycobacterium tuberculosis H37 Ra (Difco, Detroit, USA) at a concentration of 10 mg/ml. Six-week-old male Lewis rats were immunized by subcutaneous injection of 2 mg of purified cardiac myosin in each rear footpad on days 1 and 8 (Myo group, n = 15). In additional 15 rats, to suppress the inflammation, steroid of 6 mg was injected simultaneously with purified cardiac myosin emulsified with complete Freund's adjuvant

supplemented with mycobacterium tuberculosis H37 Ra (MyoS group, n = 15). The control rats received injections of 0.5 ml of complete Freund's adjuvant in the same manner (Control group, n = 15). Ambulatory Holter monitoring was performed using telemetry system (Telemetry research, Auckland, New Zealand).

2. Histology and assay of inflammatory cytokines

After measuring the hemodynamic parameters, hearts were immediately separated and weighed. The ratio of heart weight to body weight was calculated. The hearts were stained with Hematoxylin and Eosin. Immunostaining was done using tumor necrosis factor-α (TNF-α) antibody to identify the degree of inflammation.

Blood was obtained from the abdominal aorta of each group rats on day 21. Enzyme-linked immunosorbent assay was performed to determine levels of high-mobility group protein B1 (HMGB1), interleukin-6 (IL-6), and TNF-α in serum. According to the manufacturer′s instructions, protein levels in serum were quantified with HMGB1 (IBL International, Hamburg, Germany), IL-6 (R&D System, Minneapolis, MN, USA) and TNF-α (R&D System, Minneapolis, MN, USA) kits.

The immunoblotting of HMGB1, IL-6, and TNF-α were performed to evaluate the inflammation of tissue. Targeted antigens were probed with the following primary antibodies: anti-HMGB1 (Abcam Reagents, Cambridge, MA, USA), anti-IL-6 (Abcam Reagents, Cambridge, MA, USA), anti-TNF-a (Abcam Reagents, Cambridge, MA, USA) and anti-GAPDH (Santa Cruz Biotechnology Dallas, Texas, USA).

3. Optical mapping

On the 21st day after the initial immunization, rats (250 – 300 g) were anesthetized with intraperitoneal injection of ketamine (80 mg/kg) and xylazine (4 mg/kg). The chests were opened via median sternotomy and the hearts were rapidly excised and immersed in cold Tyrode′s solution (composition in mmol/L: 125 NaCl, 4.5 KCl, 0.25 $MgCl_2$, 24 $NaHCO_3$, 1.8 NaH_2PO_4, 1.8 $CaCl_2$, and 5.5 glucose). The ascending aorta was immediately cannulated and perfused with 37°C Tyrode′s solution equilibrated with 95% O_2 and 5% CO_2 to maintain a pH of 7.4. Coronary perfusion pressure is regulated between 80 and 95 mm Hg. For optical recording, the contractility of the heart was inhibited by 10-17 μmol/L of blebbistatin.[8] The hearts were stained with di-4-ANEPPS (Invitrogen, Carlsbad, CA) and excited with quasi-monochromatic light (520 ± 30 nm) from two green LED lamps. Emitting light was collected by an image-intensified charge-coupled device camera (Dalsa Inc., Waterloo, Canada) with a 610-nm long pass filter. Data was gathered at 3.75 ms sampling intervals, acquiring simultaneously from 125 x 125 pixels, each 0.08 mm x 0.08 mm. The mapped area included parts of the right and left ventricular free walls.

Optical mapping were performed in 6, 6 and 6 rats in the control, Myo and MyoS group, respectively. To evaluate the effect of CaMKII activation on arrhythmia, optical mapping was performed in additional rats with myocarditis after active CaMKII blockade (KN 93, 1 μmol/L) infusion for 20 min (Myo+KN93 group, n=5) or inactive CaMKII blockade (KN 92, 1 μmol/L) infusion for 20 min (Myo+KN92 group, n=5).

Activation and repolarization time points at each site were determined from fluorescence (F) signals by calculating $(dF/dt)max$ and $(d^2F/dt^2)max$, which has been shown to coincide with ~97% repolarization to baseline and recovery from refractoriness.[9] Action potential duration was measured from $(dF/dt)max$ to 90%

recovery to baseline, APD_{90}. Mean APD_{90} was calculated for each heart by averaging APD_{90} from a region of atrium consisting of 10x10 pixels or 100 APD_{90} from each heart for a minimum of 5 hearts. APD dispersion is defined as the difference between maximum and minimum APDs. Local conduction velocity (CV) vectors were calculated for each pixel from the differences in activation time-points of that pixel (determined from (dF/dt)max) and its 7 × 7 nearest neighbors, as previously described.[9] Local CVs were averaged and calculated as means ± standard deviation (SD). Local CV can be overestimated when two wave fronts collide, transmural propagation breaks through the surface, or when activation appears synchronous over a region of the atrium because of its proximity to the pacing electrode. To avoid overestimations of CVs, CVs > 1.25 m s^{-1} were deleted from the analysis.[10] Time and frequency domains analysis was achieved, as previously described.[11] APD Restitution Kinetics (RK) curves were generated by plotting mean APD_{90} (from a minimum of 100 pixels per atrium times a minimum of 5 hearts (right or left atria)) versus S1-S2 interval in milliseconds. CV RK curves were generated by plotting the mean CV from a minimum of 5 ventricles vs. S_1-S_2 interval in milliseconds.

4. Programmed stimulation

To test VT vulnerability, each heart was paced at the LV using a programmed stimulation protocol consisting of 20 S_1 pulses at 250 ms cycle length (CL) followed by a premature S_2 pulse with progressively shorter S_1-S_2 interval steps: 250 to 100 ms in 20 ms steps; 100 to 70 ms in 10 ms steps and 60 to 35 in 5 ms steps, until loss of capture or the initiation of VT. Optical mapping and VT induction studies were performed in 5 rats in each group.

5. Immunoblot analysis of oxidative stress markers and Ca^{2+} handling proteins

The immunoblotting of inducible nitric oxide synthase (iNOS), cyclooxygenase-2 (Cox-2), CaMKII, ryanodine receptor type 2 (RyR2), phospholamban (PLB) and phosphated form were performed by monoclonal antibodies for anti-CaMKII, anti-p-CaMKII (Santa Cruz Biotechnology Dallas, Texas, USA), anti-RyR2 (Abcam Reagents, Cambridge, MA, USA), anti-p-RyR2 (Badrilla, Leeds, UK) and anti-p-PLB (Santa Cruz Biotechnology Dallas, Texas, USA). The phosphorylation sites for CaMKII, RyR and PLB were Thr-287, Ser-2814 and Thr-17, respectively. Targeted antigens were visualized with the suitable HRP conjugated secondary IgG (Santa Cruz Biotechnology Dallas, Texas, USA) followed by enhanced chemiluminescence assay (ECL Plus, Amersham, Piscataway, NJ). Bands were scanned and their intensities were quantified with Image J software.

6. Measurement of cytosolic Free Ca^{2+}

Myocytes with myocarditis was produced by TNF-α treatment and used in intracellular calcium measurement. The measurement of the cytosolic free Ca^{2+} concentration was performed by confocal microscopy analysis. Rat cardiomyocytes were plated on a slide chamber coated with 1.5% gelatin for 1 day in α-MEM containing 10% fetal bovine serum (Gibco, Paisley, Scotland) and 0.1 μM BrdU (Sigma Aldrich, Schnelldorf, Germany). After incubation, cells were washed with modified Tyrode Tyrode′s solution (composition in mmol/L: 125 NaCl, 4.5 KCl, 0.25 $MgCl_2$, 24 $NaHCO_3$, 1.8 NaH_2PO_4, 1.8 $CaCl_2$, and 5.5 glucose). Cells were then loaded with 10 μmol/l

acetoxymethyl ester fluo-4 (Fluo-4 AM, Molecular Probe) for 20 min, at 37°C, in the dark. Fluorescence images were collected using confocal microscope excited by a 488-nm argon laser and emitted light was collected through a 510-560 nm band-pass filter. The relative intracellular Ca^{2+} concentration was determined by measuring fluorescent intensity.

7. Statistical analysis

Data were expressed as the mean ± SEM. Student's *t* tests with Bonferroni's correction were used to compare the means of two numeric values. The Pearson's chi-square tests were used to compare two categorical variables. P values <0.05 were considered statistically significant.

Ⅲ. Results

1. Arrhythmia and survival of EAM

The heart weights were were 1.2 ± 0.1 g, 1.5 ± 0.1 g and 1.3 ± 0.0 g in the control, Myo group and MyoS group, respectively (Figure 1A). The ratios of heart weight to body weight were 3.2 ± 0.3, 4.0 ± 0.5 and 3.6 ± 0.6, respectively. The Myo group had heavier heart weight than the control (p=0.001) and the MyoS group (p=0.03). The ratios of heart weight to body weight were also larger in the Myo group than the control (p=0.006).

Figure 1B shows the histological analysis on 21 days after the initial immunization with cardiac myosin. While no inflammatory changes were observed in the control rats, there was infiltration of inflammatory cells, including giant cells mainly in the right ventricle and epicardial layer of LV in Myo rats. The infiltration of inflammatory cells was not observed in MyoS group (upper and middle panels of Figure 1B). Myo rats showed increased TNF-α than control (34 ± 7% vs. 52 ± 5%, p=0.005). However, MyoS group showed significantly decreased TNF-α than Myo group (31 ± 3%, p=0.001, lower panels of Figure 1B).

Figure 1C shows the Kaplan-Meier survival curves of the three groups. While 4 (27%) out of 15 rats died suddenly at 12 ± 3 days after myocarditis in the Myo group, no (0%) rats and one (6%) rat died in the control and MyoS groups, respectively. The Myo group had a lower survival rate than the control (p=0.03). Figure 1D shows ventricular premature beat and VT recorded by ambulatory Holter monitoring in Myo group. While arrhythmias were not observed in control rats, they were observed in 5 (56%) of the 9 surviving rats and 0 (0%) of 14 survival rats from Myo and MyoS groups, respectively (p=0.03).

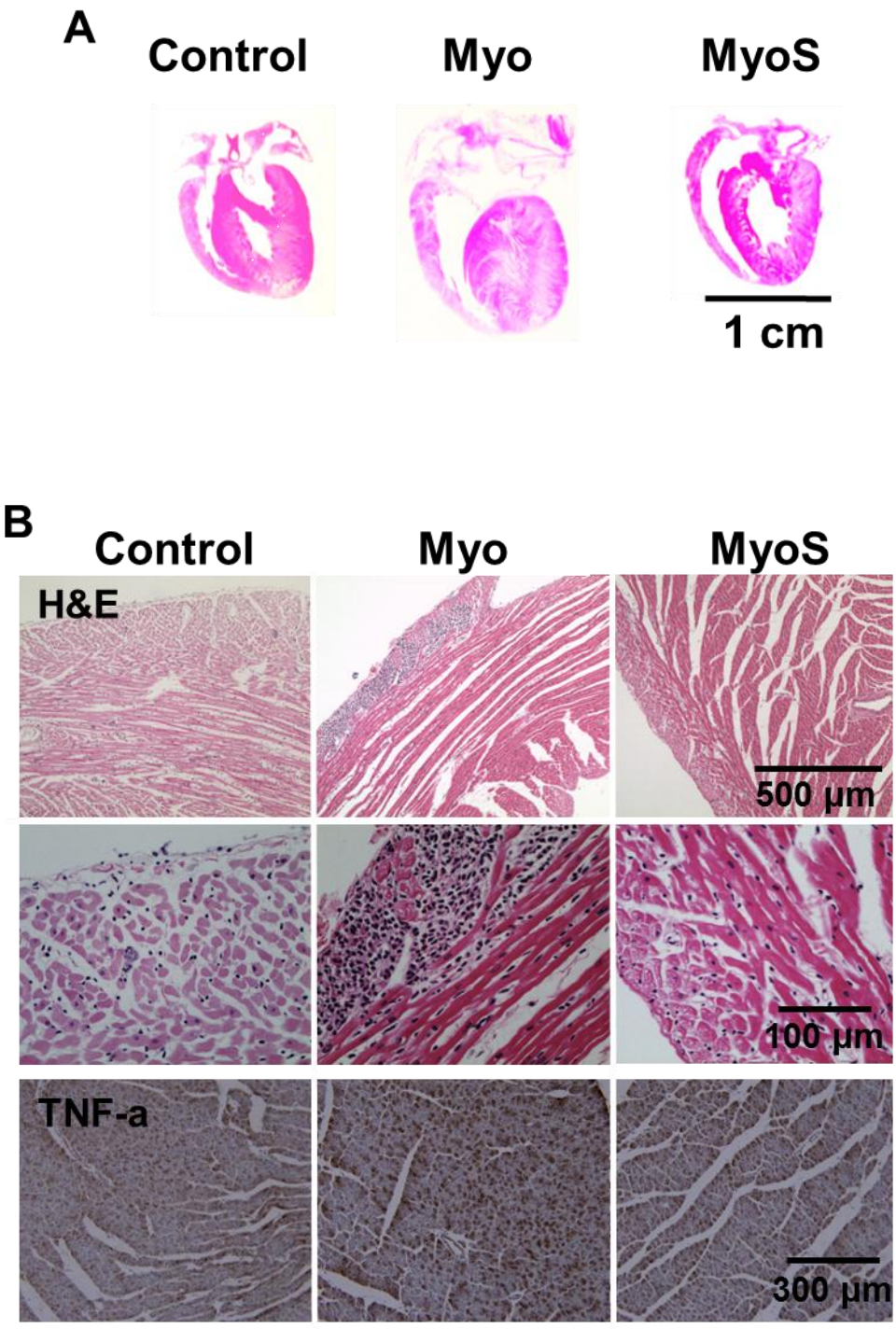
A
Control
Myo
MyoS
1 cm
B
Control
Myo
MyoS
H&E
500 μm
100 μm
TNF-a
300 μm

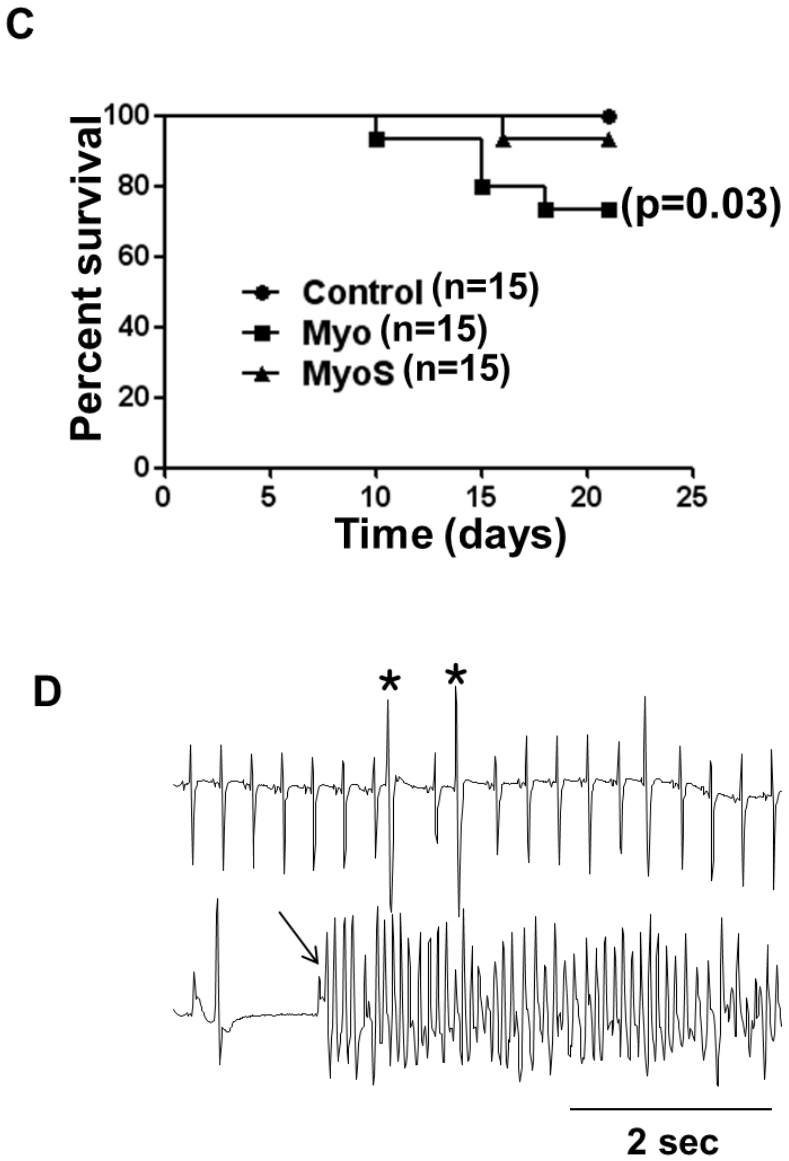

Figure 1. Histologic findings, arrhythmia and survival of EAM.

A, Gross picture of heart of the 3 groups. B, Histological analysis on 21 days after the immunization. Hematoxylin-eosin (HE) staining shows inflammation and fibrosis. Note the increased inflammation (upper and middle panels) and TNF-α expression (lower panels) in the Myo group. C, Kaplan-Meier Survival curves. The Myo group showed lower survival rate than the control (p=0.03). D, Ambulatory Holter monitoring in the

Myo group showing PVCs and VF. PVCs were marked with asterisks. The initiation of VF was marked with an arrow.

2. Increased inflammation in EAM

Compared with the control, HMGB1, IL-6 and TNF-α of the Myo group were increased by 3.1 ± 0.1 ($p<0.001$), 2.8 ± 0.4 ($p=0.003$) and 2.5 ± 0.1 ($p=0.005$) times, respectively (Figure 2A). Compared with the control, Myo group had increased serum level of HMGB1 (11.6 ± 0.2 vs. 45.0 ± 2.3 ng/ml, $P<0.001$), IL-6 (48.5 ± 8.4 vs. 97.6 ± 35.8 pg/ml, $p<0.001$) and TNF-α (16.2 ± 0.3 vs. 18.0 ± 0.6 pg/ml, $p<0.001$) (Figure 2B). However, these inflammatory markers were not increased in the MyoS group.

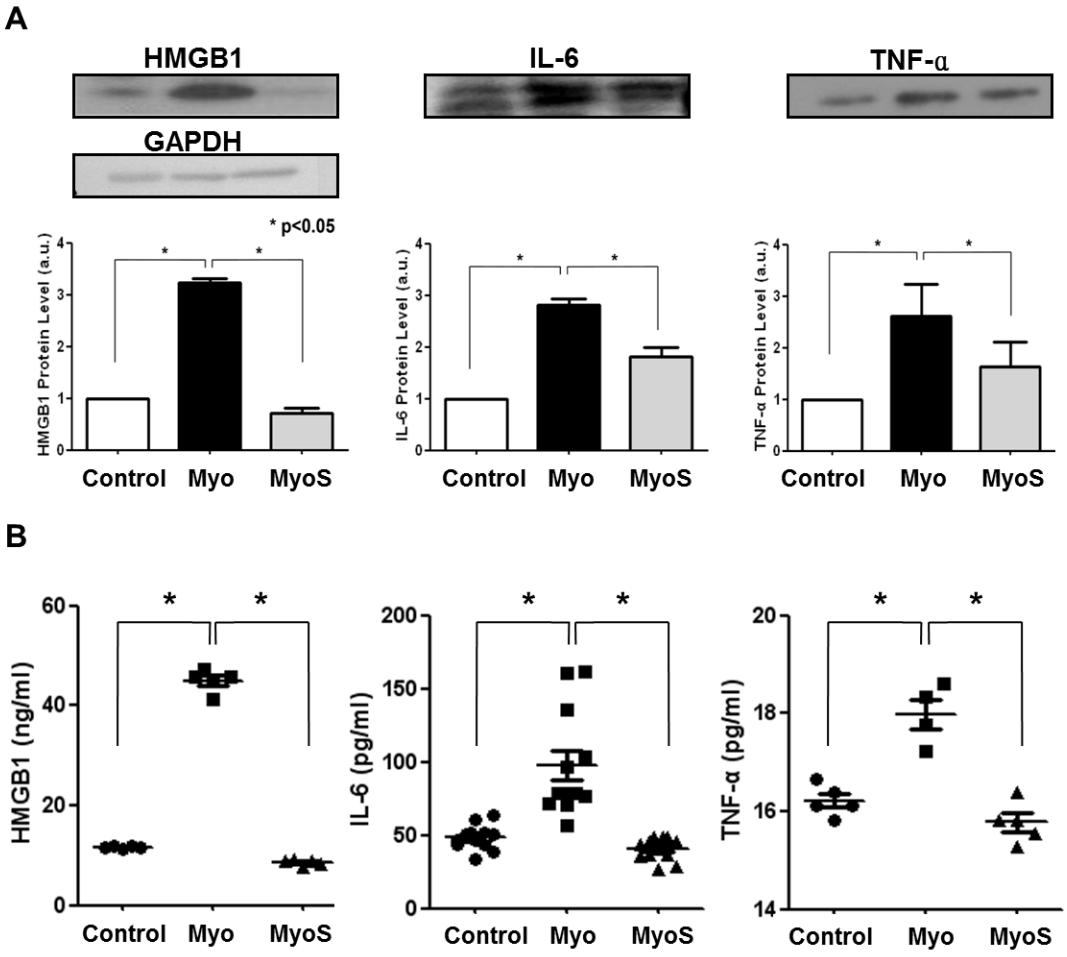

Figure 2. Inflammation in EAM.

Western blot (A) and ELISA analysis (B) of HMGB1, IL-6, TNF-α in EAM.

3. Increased APD and APD dispersion in EAM

Figure 3A shows the action potential traces at the base of LV during pacing CLs of 300 ms in Langendorff-perfused rat hearts. The Myo group had longer APD than the control and MyoS group. To evaluate the relationship between myocarditis-induced arrhythmia and CaMKII activation, we recorded action potential after the pretreatment of CaMKII inhibitor. Myocarditis induced APD prolongation was prevented by the pretreatment of KN 93 (1 μmol/L) for 20 min, but not by KN 92 (1 μmol/L) for 20 min. The comparisons of mean APD_{90} among groups were presented in Figure 3B. Myo group had a longer mean APD_{90} than the control and MyoS group at all pacing CLs. Figure 3C shows the activation and repolarization maps. Compared with the control and MyoS group, the Myo group had the crowing of activation isochronal lines, suggesting increased conduction time of ventricle. Compared with the control (13 ± 4 ms), APD dispersion was increased in the Myo group (43 ± 16 ms, p=0.001), but not in the MyoS group (17 ± 5 ms, p=1.0).

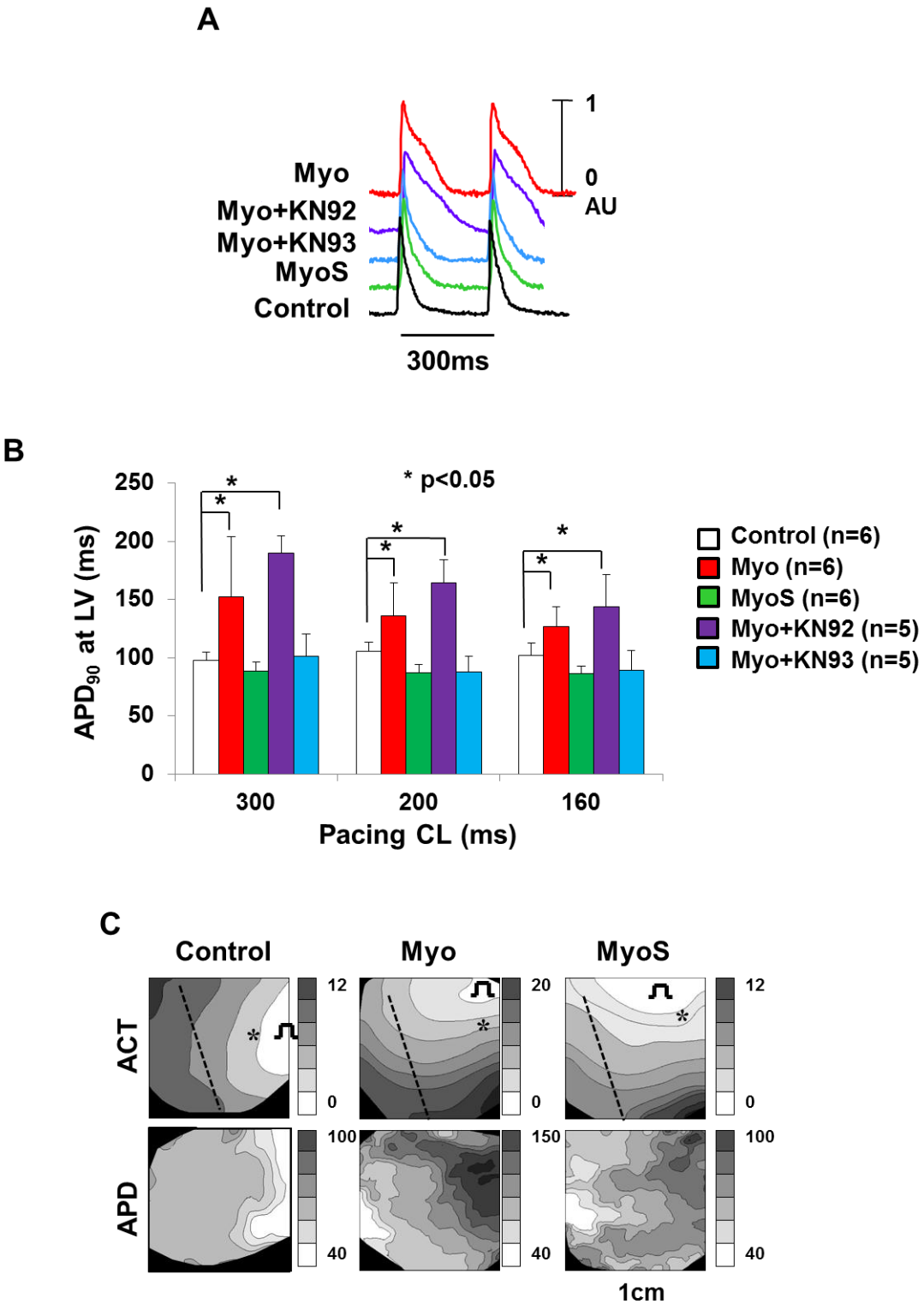
A
1
0
AU
Myo
Myo+KN92
Myo+KN93
MyoS
Control
300ms
B
* p<0.05
APD90 at LV (ms)
250
200
150
100
50
0
300
200
160
Pacing CL (ms)
Control (n=6)
Myo (n=6)
MyoS (n=6)
Myo+KN92 (n=5)
Myo+KN93 (n=5)
C
Control
Myo
MyoS
ACT
APD
12
0
20
0
12
0
100
40
150
40
100
40
1cm

Figure 3. Increased APD and APD dispersion in EAM. A, Typical action potential traces of the control (black), MyoS (green), Myo+KN93 (blue), Myo+KN92 (purple) and Myo (red) groups at the pacing CLs of 300 ms. Action potential recording sites were marked with asterisks in Figure C. B, The comparison of APD_{90} among various groups. Compared with control, APD_{90} was significantly prolonged in the Myo and Myo+KN92 groups ($p<0.05$). C, Activation (upper panels) and APD maps (lower panels). The dotted line marks the interventricular septum.

4. Increased ventricular arrhythmias in EAM

Spontaneous triggered activities were observed in 1 (17%), 5 (83%) and 2 (33%) rats in the control (n=6), Myo group (n=6) and MyoS group (n=6). Spontaneous triggered activities were more frequently observed in Myo group than in control group (p=0.02). By programmed stimulation, ventricular arrhythmia including VT or VF was induced in all (100%) rats with EAM (Myo group). However, no and 1 (17%) rat had inducible ventricular arrhythmia in control and MyoS group, respectively. Ventricular arrhythmias were more frequently induced in Myo group than in control (p=0.001) and in MyoS group (p=0.003).

Figure 4 shows an example of spontaneous triggered activity and VT observed in an EAM model. Beats #1-3 each had the same normal conduction pattern, originating from the left upper side of recording window, while beat #4 was a spontaneously triggered beat originating from apex of the LV (site 2). Beat #5 had also the same normal conduction pattern. The subsequent 3 beats (#6-9) also originated from the same site (site 2).

5. Increased VT Vulnerability in EAM

The typical examples of induced VF were presented in Figure 4C. VT were induced in 0, 4 (80%), and 0 (0%) rats in control (n=5), Myo (n=5), and MyoS (n=5), respectively. Myocarditis hearts had higher inducible VT or VF than control (p=0.01). Steroid treatment prevented inducible VT or VF after myocarditis (p=0.01). Inducible ventricular arrhythmias were not observed in the Myo+KN 93 group, but in 2 out of 3 hearts from the Myo+KN 92 group. Myo+KN 93 group showed significantly lower incidence of spontaneous triggered activities (p=0.02) than Myo group.

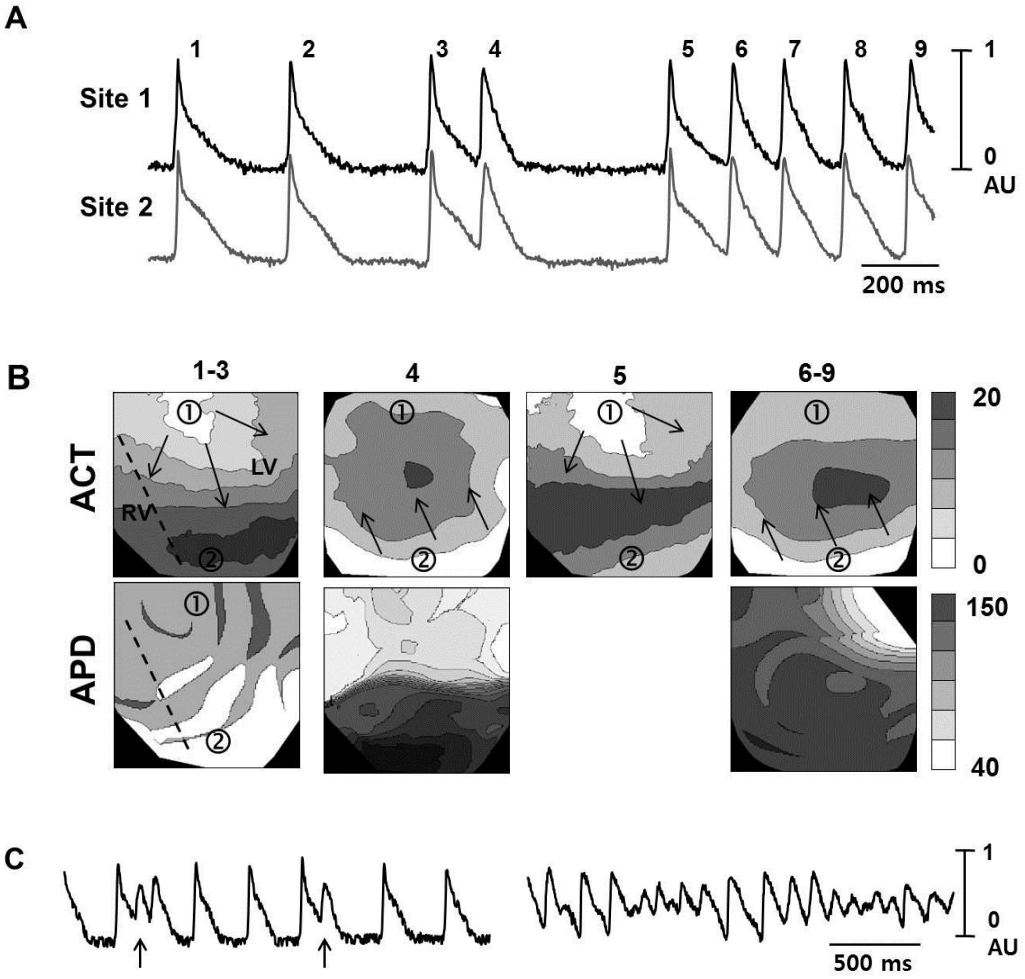

Figure 4. Spontaneous triggered activity and VT in EAM. A, The action potential tracings from base (site 1, black) and apex (site 2, gray) of LV showing triggered activity and VT. B, The activation maps show the first three beats originating from the LV base (site 1). The fourth beat was generated from apex of LV (site 2), after which the fifth beat was originated from the same site as the 1–3rd beats. Beats #6-9 were generated from the LV apex (site 2). The dotted line marks the interventricular septum. C, Other examples of spontaneous triggered activity (left, arrows) and VF (right) in EAM.

6. Increased spatially discordant alternans and restitution kinetics in EAM

Spatially discordant alternans were easily induced in Myo group. Figure 5A shows a typical example of action potential traces of the control, Myo and MyoS groups at various pacing heart rates. The discordant alternans (asterisks of Figure 5A) were observed at the heart rate of 750 bpm, 460 bpm and 600 bpm in the control, Myo group and MyoS group, respectively. For the control, Myo and MyoS group, the discordant alternans heart rate threshold were 673 ± 76 bpm, 306 ± 34 bpm and 527 ± 25 bpm, respectively (Figure 5B). Compared with control ($p<0.001$) and MyoS group ($p=0.01$), the Myo group showed significantly decreased the heart rate at which discordant alternans is elicted. Conduction block and reentry were also observed after lower heart rate in the Myo group than other groups (Figure 6).

CV and APD restitution kinetics (RK) were measured from the both ventricles of control, Myo and MyoS. While myocarditis increased the steepness of APD RK curve, steroid treatment reversed the slope of APD RK curves at both ventricles (Figure 7A and 7C). Steroid-treated myocarditis hearts had shorter APD_{90} RK curves compared with myocarditis hearts, consistent with $APD_{90.}$ Figure 7B shows a marked effect of steroid on the CV RK compared with myocarditis hearts—namely, a large increase in CV particularly for short S1–S2 intervals and a less-steep RK curve. The slower CV of the premature pulse and of the first spontaneous reentrant beat in myocarditis ventricle helps to sustain VT.

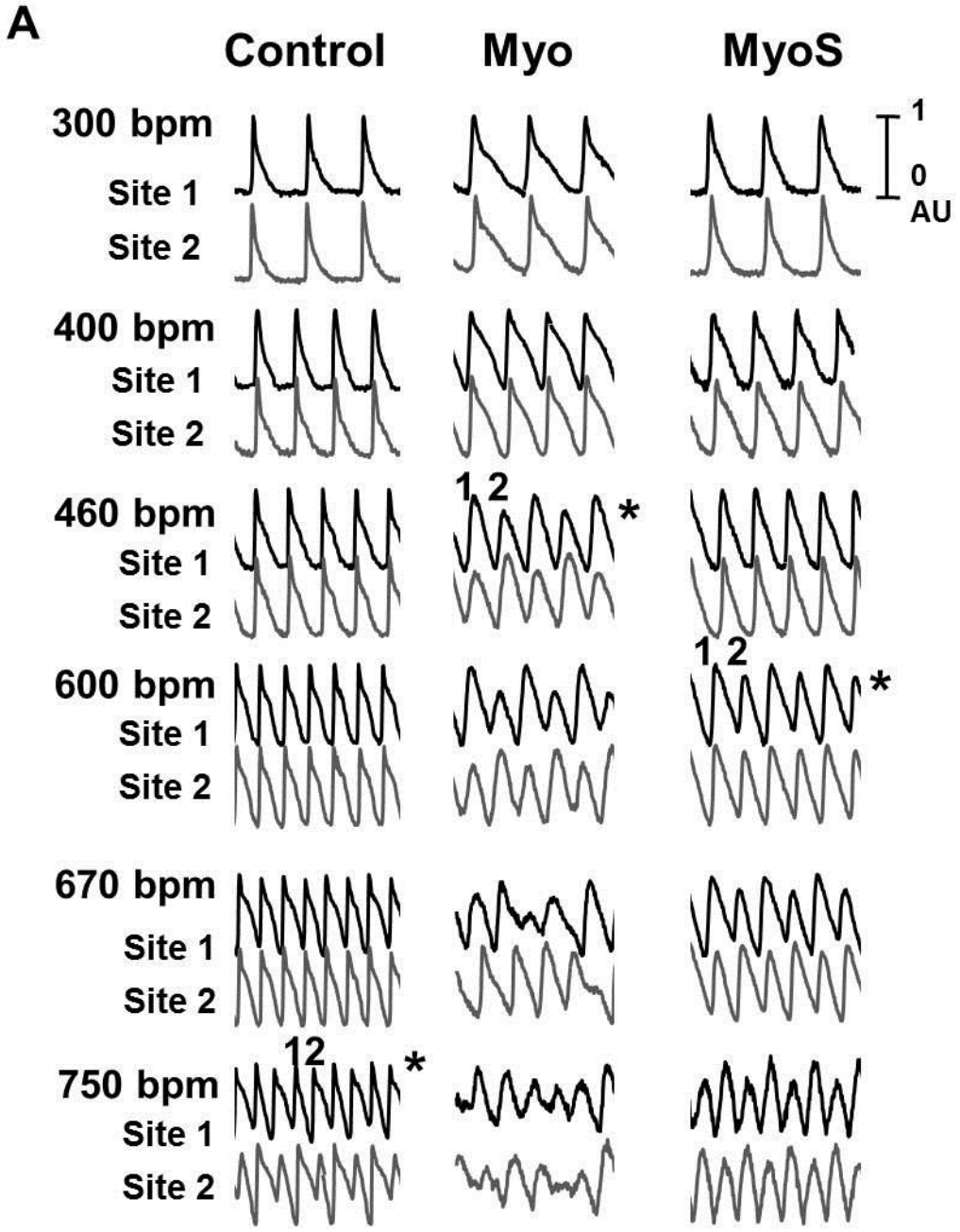
A
Control
Myo
MyoS
300 bpm
Site 1
Site 2
1
0
AU
400 bpm
Site 1
Site 2
460 bpm
Site 1
Site 2
1 2
*
600 bpm
Site 1
Site 2
1 2
*
670 bpm
Site 1
Site 2
750 bpm
Site 1
Site 2
1 2
*

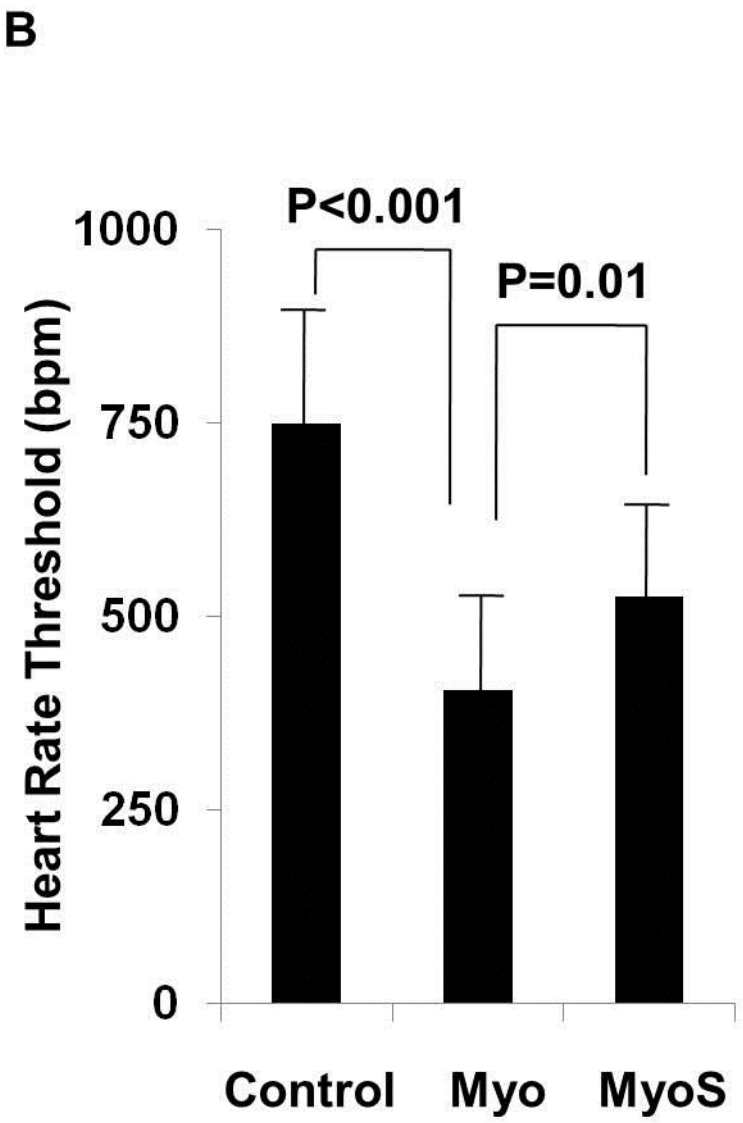

Figure 5. Aggravated spatially discordant alternans in EAM. A, Action potential traces of control, Myo and MyoS group at various pacing heart rates. B, Spatially Discordant Alternans at the pacing heart rates of 750 bpm, 460 bpm and 600 bpm in the control, Myo and MyoS group, respectively.

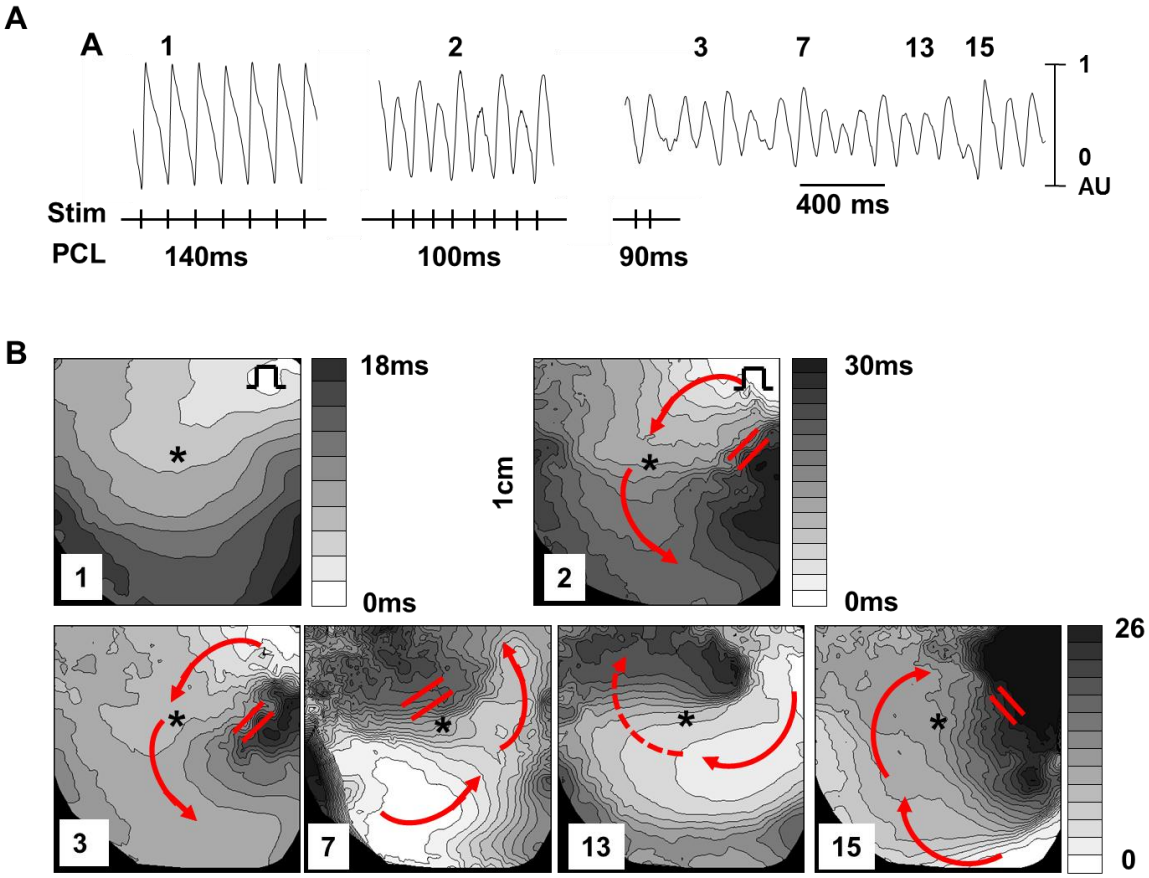

Figure 6. Initiation of epicardial reenty and VF in myocarditis. A, Action potential traces during pacing CL of 140 ms, 110 ms and 90 ms in myocarditis model. The recording sites are marked in Figure B. B, Activation maps. The activation wave front of beat #1 propagated uniformly from the stimulation site. Beat #2 blocked at the lateral part left ventricle, as represented by hatched area in activation map. Note the discordant alternans on beat #2. Beats #3-4 show the epicardial reentry. The beat #5-6 were activated reversely from beat #3-4.

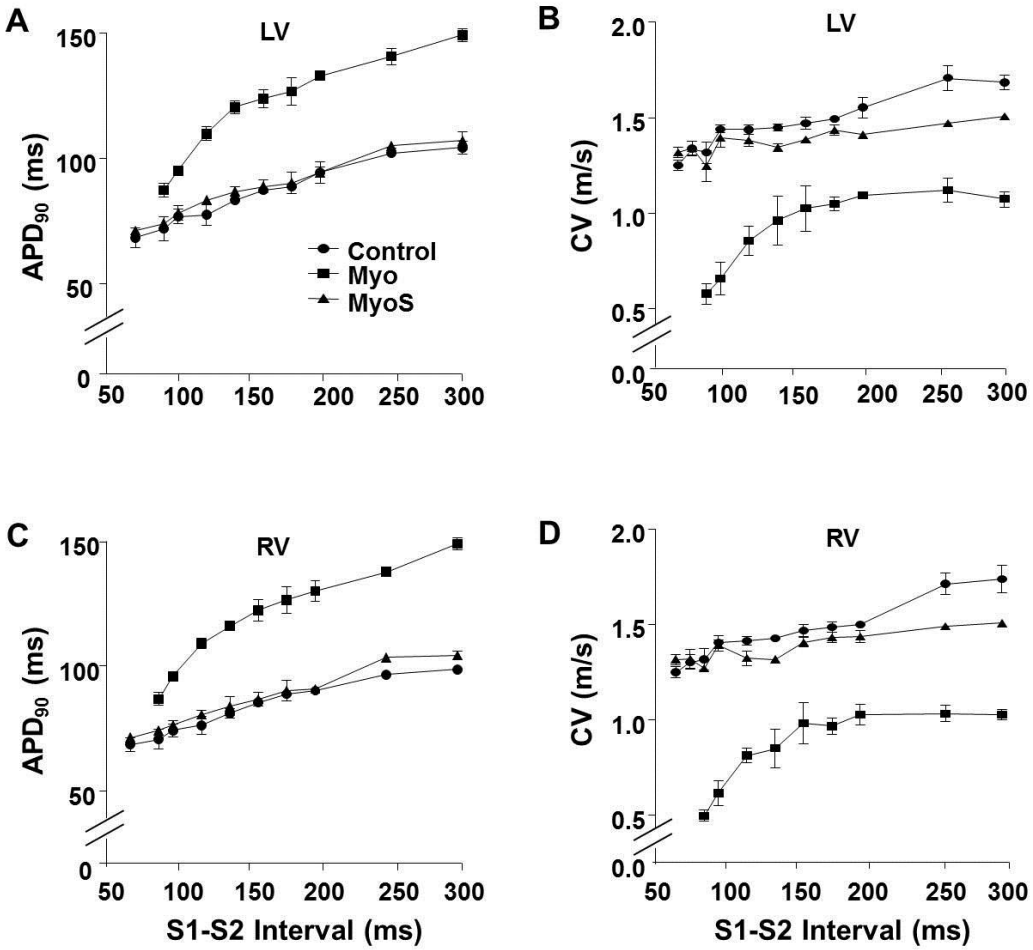

Figure 7. Restitution kinetics(RK) of APD and CV. A and B, RK measured from the left ventricle for APDs at 90% recovery to baseline(APD_{90}) and CV, respectively. C and D, RK measured from right ventricle for APD_{90} and CV. CV and APD90 were measured as a function of S1− S2 interval.

7. Cytosolic Free Ca^{2+}.

Next, alterations in impaired intracellular calcium were examined, because focal activity is easily induced by Ca^{2+} overload in a myocarditis setting. Myocytes with myocarditis produced by TNF-α treatment used in intracellular calcium measurement. A significant increase in fluorescence intensity was seen in myocarditis cardiomyocytes, indicating Ca^{2+} overload (Figure 8A). However, pretreatment with steroid or KN93 decreased the fluorescence intensity by 1.3 times compared with Myo group (Figure 8B).

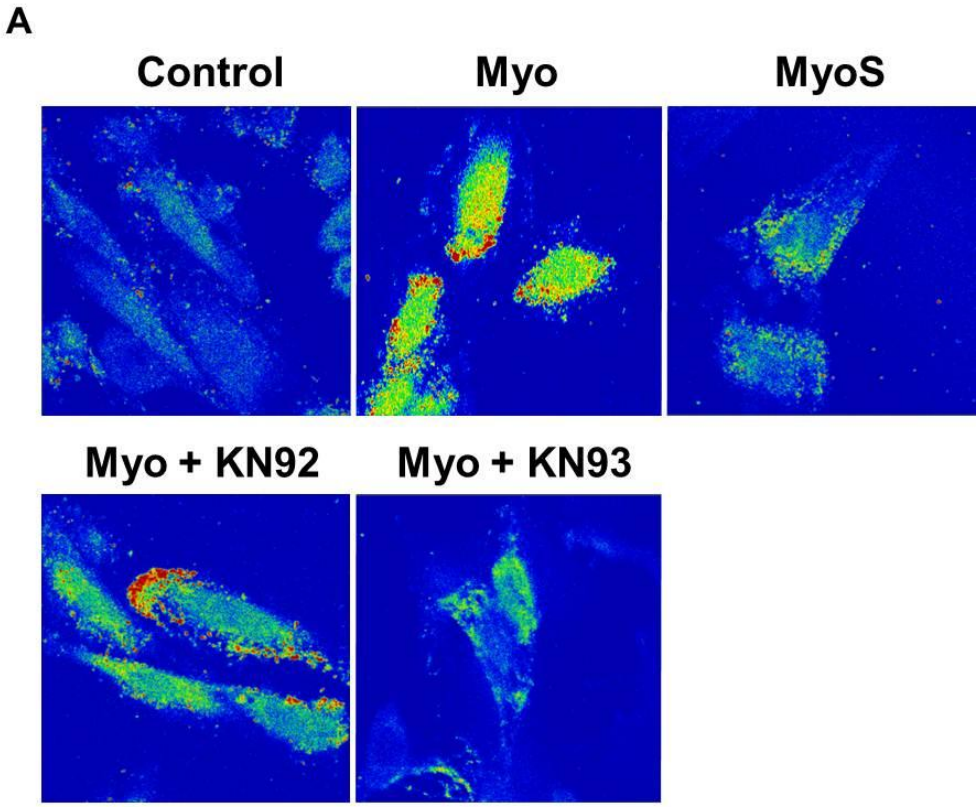
A
Control
Myo
MyoS
Myo + KN92
Myo + KN93

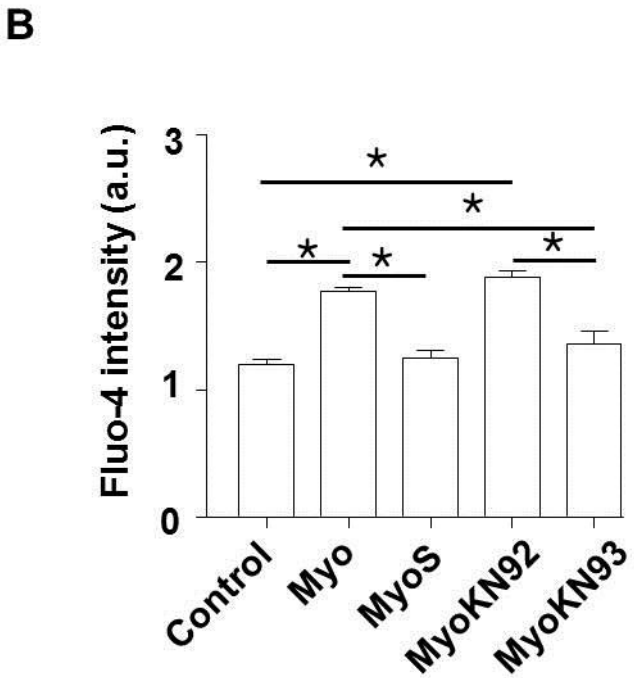
B
Fluo-4 intensity (a.u.)
3
2
1
0
*
*
*
*
*
Control
Myo
MyoS
MyoKN92
MyoKN93

Figure 8. Intracellular Ca^{2+} concentration in EAM. A, Representative fluorescent images of cytosolic free Ca^{2+}. B, Relative fluorescence intensity in Control, Myo, MyoS, Myo KN92 and Myo KN93. (*$p<0.01$)

8. Increased p-CaMKII, RyR2 and p-PLB in EAM

EAM significantly increased oxidative stress and Ca^{2+} handling proteins (Figure 9A). Compared with control, iNOS and Cox-2 were increased in Myo group. However, the increase of iNOS and Cox-2 was prevented by steroid pretreatment (MyoS group).

Compared with the control, p-CaMKII, RyR2, p-RyR2 and p-PLB of the Myo groups were increased by 2.5 ± 0.3 ($p<0.001$), 2.9 ± 0.1 ($p<0.001$), 5.1 ± 0.2 ($p<0.001$) and 2.3 ± 0.1 ($p<0.001$) times, respectively. However, they were not increased in MyoS group (Figure 9B).

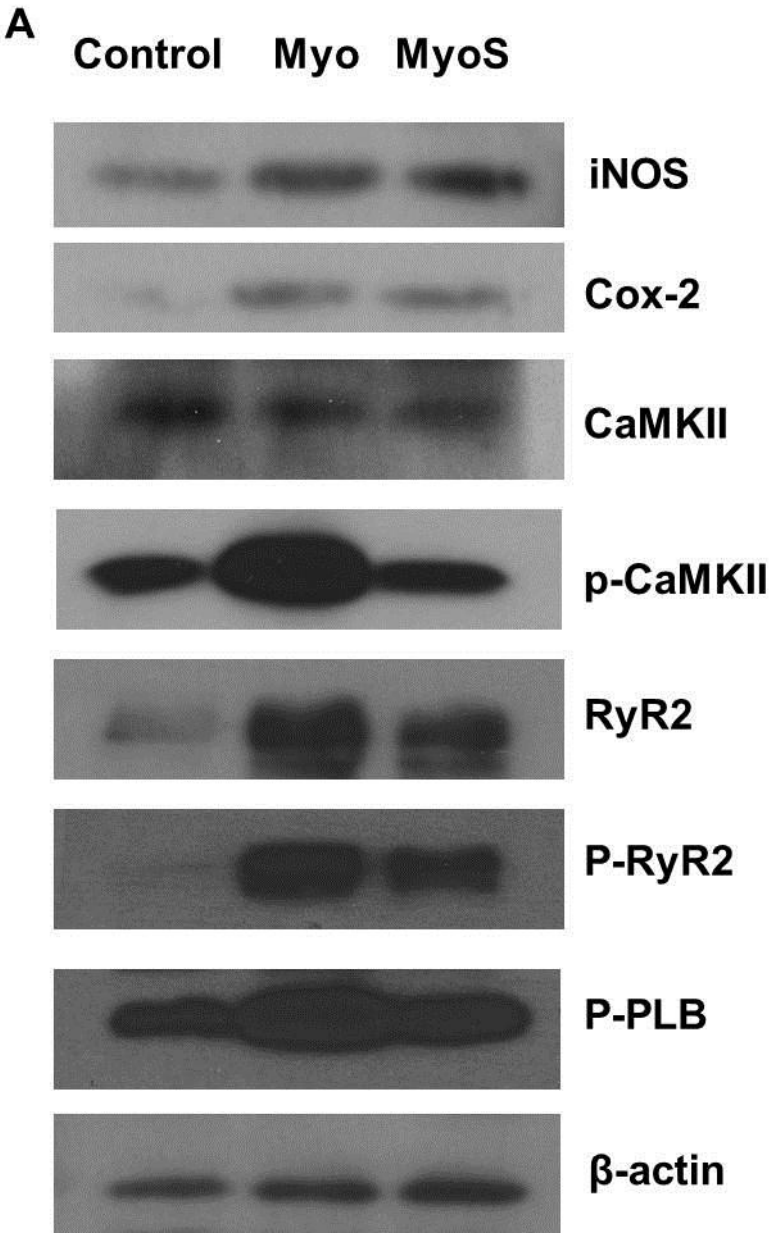
A
Control
Myo
MyoS
iNOS
Cox-2
CaMKII
p-CaMKII
RyR2
P-RyR2
P-PLB
β-actin

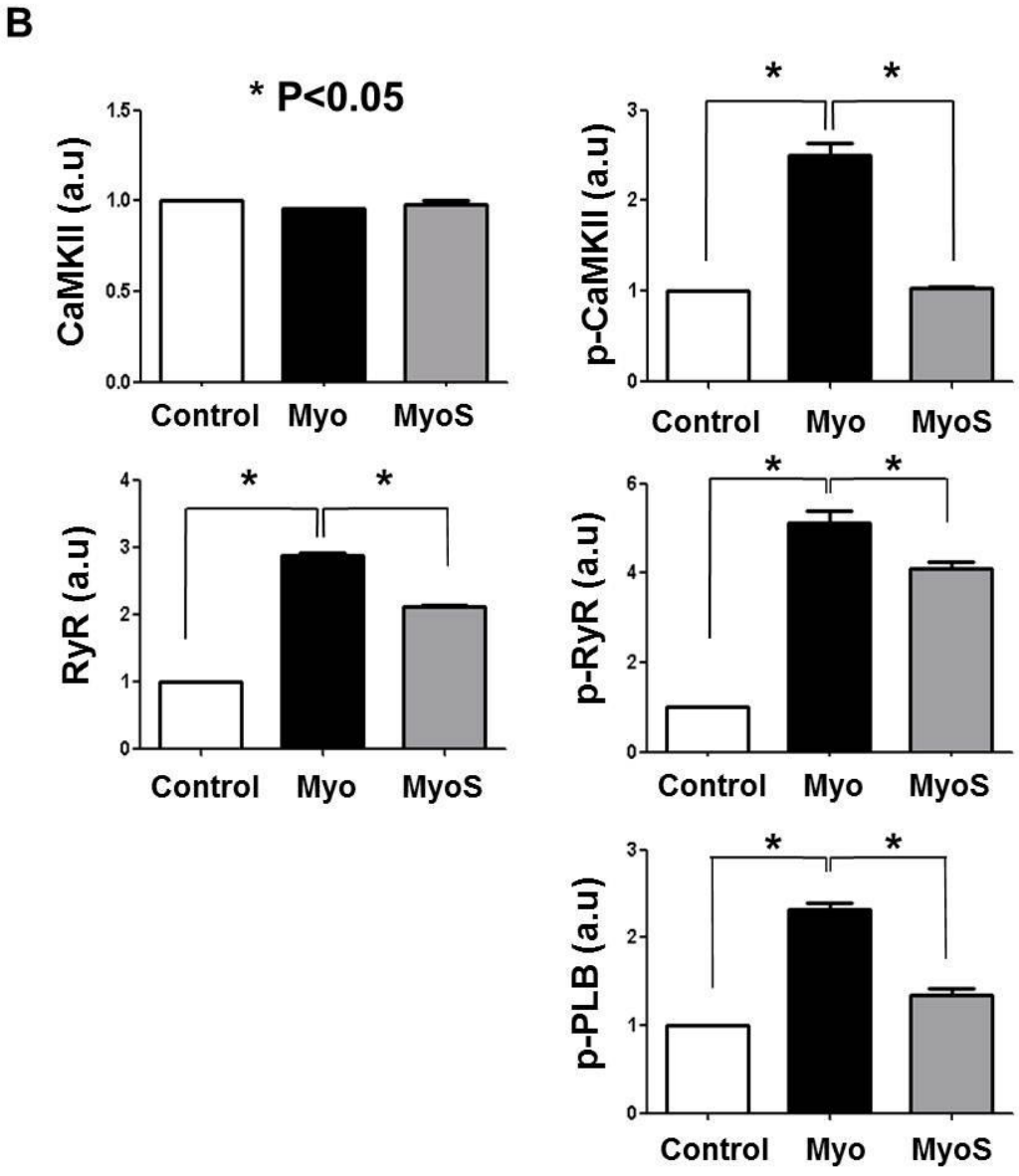

Figure 9. Western blot assay of oxidative stress and Ca^{2+} handling protein. A, Western blot analysis. B, The quantification showing increased p-CaMKII, RyR2, p-RyR2 and p-PLB in EAM. However, they were not increased in the MyoS group. P-values less than 0.05 were marked with asterisks.

Ⅳ. Discussion

1. Main findings

Firstly, the rats with EAM showed decreased survival and fatal ventricular tachyarrhythmia. Secondly, the EAM model showed electrophysiological characteristics of increased APD dispersion and spatially discordant alternans, and steeper restitution slope. Spontaneous triggered activity and VT inducibility were increased in EAM. Thirdly, the EAM model had increased activity of calcium handling proteins, including p-CaMKII, p-RyR2 and p-PLB. Finally, the EAM related arrhythmias and the activation of calcium handling proteins were attenuated by steroid pretreatment. Our results suggest that the mechanism of arrhythmia in EAM might be related with the increased phosphorylation of Ca^{2+} handling protein caused by the inflammation and oxidative stress.

2. Increased repolarization gradient and CaMKII activation in EAM

Abundant evidence now supports an important role of CaMKII in promoting heart failure and arrhythmias by actions on SR Ca^{2+} uptake and release.[12] The mechanism of CaMKII hyperactivity in heart failure is likely attributable to either autophosphorylation of threonine 287 and/or oxidation of methionines 281 and 282.[13] In this study, we found that the phosphorylation of CaMKII at Thr 287 was increased in myocarditis, suggesting mechanism of CaMKII hyperactivity attributable to autophosphorylation of threonine 287.

RyR2 is a SR Ca^{2+} release channel that is activated by a trigger of Ca^{2+} from ICa.[14] RyR2 phosphorylation by protein kinase A and CaMKII both enhance ICa and RyR2 Ca^{2+} release. CaMKII helps coordinate this physiological process of Ca^{2+}-induced Ca^{2+} release by phosphorylation of CaV1.2 and RyR2. However, in failing myocytes the cell membrane ultrastructure supporting Ca^{2+}-induced Ca^{2+} release is distorted [15] and CaMKII hyperphosphorylation of CaV1.2 and RyR2 becomes arrhythmogenic. In this study, myocarditis had CaMKII hyperphosphorylation of serine 2814 on RyR2. CaMKII hyperphosphorylation of serine 2814 on RyR2 promotes RyR2 Ca^{2+} leak and arrhythmia-triggering delayed afterdepolarizations [16] while depleting SR Ca^{2+} to impair inotropy.[17-21] PLB is a negative regulator of SERCA [22], but PLB phosphorylation by protein kinase A (at serine 16) or CaMKII (at threonine 17) can reduce the inhibitory efficacy of PLB, leading to increased SERCA activity. In this study, PLB was phosphorylated at Thr-17 in myocarditis.

Previous studies reported the initial reduction of I_{to}-related molecules, such as the expression levels of Kv4.2, Kv1.5, frequenin and KChIP2 in EAM model.[23,24] However, the role of Ca^{2+} handling protein has not been evaluated in EAM. To our knowledge, our result suggests that the activation of Ca^{2+} handling protein might be one of the mechanisms in EAM-induced arrhythmias.

3. The mechanism of ventricular arrhythmia in EAM

In this study, the EAM model showed electrophysiological features characterized by increased APD and APD dispersion. Although APD prolongation is the main mechanism of long QT syndrome, enhanced dispersion of repolarization is critical to induce fatal arrhythmia.[25] Transmural and apicobasal dispersion of repolarization was

shown to be responsible for the initiation of reentrant activation in long QT syndrome patients. An increased spatial dispersion of repolarization across the anterior epicardial surface was also demonstrated as the electrical basis for spontaneous malignant arrhythmias in long QT type 2 rabbits.[26]

Another interesting electrophysiological finding of EAM model was the increased spatially discordant alternans. Spatially discordant alternans cause an increase in the spatial dispersion in the repolarization, and is thought to result in T-wave alternans.[27] T-wave alternans are a precursor of cardiac electrical instability and consequently sudden cardiac death.[28] Spatially discordant alternans can be explained by the increased steepness of APD restitution slope in EAM. A steep slope of electrical restitution predisposes to the breakup of single spiral waves into multiple spiral waves, a process that may account for the transition from VT to VF.[29,30] Especially, the slope of the electrical restitution ≥1 is related with VF.[31] Secondly, the discordant alternans can be related with altered Ca^{2+} handling protein. The net effects of EAM remodeling promote Ca^{2+} alternans via phosphorylating RyRs and CaMKII signaling to increase their Ca^{2+} sensitivity (increasing both gain and leak).[32,33]

4. The attenuation of EAM-induced arrhythmia by anti-inflammatory therapy

The inflammatory cytokines, such as HMGB-1, TNF-α or IL-6, were overexpressed in rats with EAM. As these inflammatory cytokines are strong inducers of reactive oxygen species, this inflammatory process may promote cardiac injury and electrical remodeling.[4,34] Niwano et al.[35] reported that the N-acetylcysteine treatment suppressed ventricular remodeling in the EAM rats. This study consistently showed that

steroid pretreatment was related with improved survival and the suppression of arrhythmias in rats with EAM. Therefore, the prevention of inflammation might suppress arrhythmia by preventing the remodeling or myocarditis itself.

Ⅴ. Study limitations

Previous studies reported initial reduction of I_{to}-related molecules, such as the expression levels of Kv4.2, 1.5, frequenin and KChIP2 in EAM model.[23,24] Measurements of Kv4.2, 1.5, frequenin and/or KChIP2 might help to confirm that this EAM model agrees with previously published data.

Ⅵ. Conclusion

The electrophysiologic characteristics of EAM were increased repolarization, repolarization dispersion and spatially discordant alternans. In EAM, phosphorylation of Ca^{2+} handling protein caused by the inflammation and oxidative stress was increased. These changes might be related with calcium overloading by increased phosphorylation of CaMKII and this might be one of the mechanisms of arrhythmia.

References

1. Eriksson U, Penninger JM. Autoimmune heart failure: new understandings of pathogenesis. Int J Biochem Cell Biol 2005;37:27-32.
2. Feldman AM, McNamara D. Myocarditis. N Engl J Med 2000;343:1388-98.
3. Levi D, Alejos J. Diagnosis and treatment of pediatric viral myocarditis. Curr Opin Cardiol 2001;16:77-83.
4. Kodama M, Matsumoto Y, Fujiwara M, Masani F, Izumi T, Shibata A. A novel experimental model of giant cell myocarditis induced in rats by immunization with cardiac myosin fraction. Clin Immunol Immunopathol 1990;57:250-62.
5. Erickson JR, Joiner ML, Guan X, Kutschke W, Yang J, Oddis CV, et al. A dynamic pathway for calcium-independent activation of CaMKII by methionine oxidation. Cell 2008;133:462-74.
6. Xie LH, Chen F, Karagueuzian HS, Weiss JN. Oxidative-stress-induced afterdepolarizations and calmodulin kinase II signaling. Circ Res 2009;104:79-86.
7. Inomata T, Hanawa H, Miyanishi T, Yajima E, Nakayama S, Maita T, et al. Localization of porcine cardiac myosin epitopes that induce experimental autoimmune myocarditis. Circ Res 1995;76:726-33.

8. Joung B, Tang L, Maruyama M, Han S, Chen Z, Stucky M, et al. Intracellular calcium dynamics and acceleration of sinus rhythm by beta-adrenergic stimulation. Circulation 2009;119:788-96.

9. Efimov IR, Huang DT, Rendt JM, Salama G. Optical mapping of repolarization and refractoriness from intact hearts. Circulation 1994;90:1469-80.

10. Ziv O, Morales E, Song YK, Peng X, Odening KE, Buxton AE, et al. Origin of complex behaviour of spatially discordant alternans in a transgenic rabbit model of type 2 long QT syndrome. J Physiol 2009;587:4661-80.

11. Choi BR, Nho W, Liu T, Salama G. Life span of ventricular fibrillation frequencies. Circ Res 2002;91:339-45.

12. Wehrens XH. CaMKII regulation of the cardiac ryanodine receptor and sarcoplasmic reticulum calcium release. Heart Rhythm 2011;8:323-5.

13. Swaminathan PD, Purohit A, Hund TJ, Anderson ME. Calmodulin-dependent protein kinase II: linking heart failure and arrhythmias. Circ Res 2012;110:1661-77.

14. Fabiato A. Calcium-induced release of calcium from the cardiac sarcoplasmic reticulum. Am J Physiol 1983;245:C1-14.

15. Song LS, Sobie EA, McCulle S, Lederer WJ, Balke CW, Cheng H. Orphaned ryanodine receptors in the failing heart. Proc Natl Acad Sci U S A 2006;103:4305-10.

16. Ai X, Curran JW, Shannon TR, Bers DM, Pogwizd SM. Ca^{2+}/calmodulin-dependent protein kinase modulates cardiac ryanodine receptor phosphorylation and sarcoplasmic reticulum Ca^{2+} leak in heart failure. Circ Res 2005;97:1314-22.

17. Wehrens XH, Lehnart SE, Reiken SR, Marks AR. Ca^{2+}/calmodulin-dependent protein kinase II phosphorylation regulates the cardiac ryanodine receptor. Circ Res 2004;94:e61-70.

18. Rodriguez P, Bhogal MS, Colyer J. Stoichiometric phosphorylation of cardiac ryanodine receptor on serine 2809 by calmodulin-dependent kinase II and protein kinase A. J Biol Chem 2003;278:38593-600.

19. Li L, Satoh H, Ginsburg KS, Bers DM. The effect of Ca^{2+}-calmodulin-dependent protein kinase II on cardiac excitation-contraction coupling in ferret ventricular myocytes. J Physiol 1997;501 (Pt 1):17-31.

20. Guo T, Zhang T, Mestril R, Bers DM. Ca^{2+}/Calmodulin-dependent protein kinase II phosphorylation of ryanodine receptor does affect calcium sparks in mouse ventricular myocytes. Circ Res 2006;99:398-406.

21. Yang D, Zhu WZ, Xiao B, Brochet DX, Chen SR, Lakatta EG, et al. Ca^{2+}/calmodulin kinase II-dependent phosphorylation of ryanodine receptors suppresses Ca^{2+} sparks and Ca^{2+} waves in cardiac myocytes. Circ Res 2007;100:399-407.

22. Mattiazzi A, Kranias EG. CaMKII regulation of phospholamban and SR Ca^{2+} load. Heart Rhythm 2011;8:784-7.

23. Saito J, Niwano S, Niwano H, Inomata T, Yumoto Y, Ikeda K, et al. Electrical remodeling of the ventricular myocardium in myocarditis: studies of rat experimental autoimmune myocarditis. Circ J 2002;66:97-103.

24. Wakisaka Y, Niwano S, Niwano H, Saito J, Yoshida T, Hirasawa S, et al. Structural and electrical ventricular remodeling in rat acute myocarditis and subsequent heart failure. Cardiovasc Res 2004;63:689-99.

25. Antzelevitch C. Ionic, molecular, and cellular bases of QT-interval prolongation and torsade de pointes. Europace 2007;9 Suppl 4:iv4-15.

26. Brunner M, Peng X, Liu GX, Ren XQ, Ziv O, Choi BR, et al. Mechanisms of cardiac arrhythmias and sudden death in transgenic rabbits with long QT syndrome. J Clin Invest 2008;118:2246-59.

27. Pastore JM, Girouard SD, Laurita KR, Akar FG, Rosenbaum DS. Mechanism linking T-wave alternans to the genesis of cardiac fibrillation. Circulation 1999;99:1385-94.

28. Rosenbaum DS, Jackson LE, Smith JM, Garan H, Ruskin JN, Cohen RJ. Electrical alternans and vulnerability to ventricular arrhythmias. N Engl J Med 1994;330:235-41.

29. Karma A. Electrical alternans and spiral wave breakup in cardiac tissue. Chaos 1994;4:461-72.

30. Witkowski FX, Leon LJ, Penkoske PA, Giles WR, Spano ML, Ditto WL, et al. Spatiotemporal evolution of ventricular fibrillation. Nature 1998;392:78-82.

31. Riccio ML, Koller ML, Gilmour RF, Jr. Electrical restitution and spatiotemporal organization during ventricular fibrillation. Circ Res 1999;84:955-63.

32. Wehrens XH, Lehnart SE, Marks AR. Intracellular calcium release and cardiac disease. Annu Rev Physiol 2005;67:69-98.

33. Curran J, Hinton MJ, Rios E, Bers DM, Shannon TR. Beta-adrenergic enhancement of sarcoplasmic reticulum calcium leak in cardiac myocytes is mediated by calcium/calmodulin-dependent protein kinase. Circ Res 2007;100:391-8.

34. Okura Y, Yamamoto T, Goto S, Inomata T, Hirono S, Hanawa H, et al. Characterization of cytokine and iNOS mRNA expression in situ during the course of experimental autoimmune myocarditis in rats. J Mol Cell Cardiol 1997;29:491-502.

35. Niwano S, Niwano H, Sasaki S, Fukaya H, Yuge M, Imaki R, et al. N-acetylcysteine suppresses the progression of ventricular remodeling in acute myocarditis: studies in an experimental autoimmune myocarditis (EAM) model. Circ J 2011;75:662-71.

ABSTRACT (In Korean)

심근염 모델에서 Ca^{2+} Handling Protein 인산화 증가 및 부정맥 유발기전

<지도교수 정보영>

연세대학교 대학원 의과학과

박혜림

심근염은 심부전, 부정맥 등의 치명적인 증상으로 발현하여 사망에 이를 수 있는 질환이다. 하지만 아직까지 심근염 모델에서 부정맥의 발생기전에 대하여는 밝혀져 있지 않다. 본 연구는 쥐 심근염 모델에서의 부정맥 발생기전을 조사하였다. 심근염 모델은 porcine cardiac myosin (10mg/ml) 0.2 ml 를 성인 Lewis rat 에 0 일째 7 일째 발바닥에 주사하여 만들었다 (심근염군). 또한 스테로이드의 부정맥 억제 효과를 보기 위하여, corticosteroid 7mg 을 0 일째 7 일째 근육 내 주사하고 porcine cardiac myosin (10mg/ml) 0.2 ml 을 발바닥에 주사하였다. (스테로이드군). 그 결과 심근염 심장은 활동전위기간이 길었고, 전도 속도가 느렸고, 전도 속도는 가파른 restitution

kinetics, 섬유화 증가, 염증과 관련된 HMGB1, IL-6, and TNF-α 의 증가가 관찰되었다. Ca^{2+}/calmodulin-dependent protein kinase II (CAMKII), ryanodine receptor type 2 (RyR2)와 phospholamban(PLB) 인산화가 증가됨을 확인하였다. 반면에 steroid 처리는 평평한 전도 속도 restitution kinetics 와 기준선에서 90% 회복까지의 활동전위기간이 감소함을 보여주었고, 전도속도의 증가, 섬유화 감소 및 CaMKII, RyR2, PLB 의 인산화도 감소하였다. 계획 전기자극은 심근염 군에서 지속형 빈맥을 발생시켰지만, 대조군, 스테로이드 군, CaMKII 억제제 (KN93) 처리 그룹에서는 발생하지 않았다. 세포배양에서 TNF-α 를 투여하여 염증을 유발하였을 때 대조군에 비해 세포 내 칼슘이 유의하게 증가했으나 ($p<0.01$) 스테로이드와 KN93 을 처리한 군에서는 감소하였다. 심근염에서의 전기생리학적 특성은 증가된 활동전위, 느려진 전도속도, 가파른 전도속도 restitution kinetics 로 나타났다. 이러한 변화들은 CaMKII 인산화 증가로 인한 칼슘 축적과 연관된 것으로 설명할 수 있다고 본다.

핵심 되는 말: 심근염, 부정맥, 염증, Ca^{2+}/calmodulin-dependent protein kinase II